MATERIALS SCIENCE

Dual-gradient enabled ultrafast biomimetic snapping of hydrogel materials

Wenxin Fan[1]*, Caiyun Shan[1]*, Hongyu Guo[2], Jianwei Sang[1], Rui Wang[1], Ranran Zheng[1], Kunyan Sui[1†], Zhihong Nie[3,2†]

The design of materials that can mimic the complex yet fast actuation phenomena in nature is important but challenging. Herein, we present a new paradigm for designing responsive hydrogel sheets that can exhibit ultrafast inverse snapping deformation. Dual-gradient structures of hydrogel sheets enable the accumulation of elastic energy in hydrogels by converting prestored energy and rapid reverse snapping (<1 s) to release the energy. By controlling the magnitude and location of energy prestored within the hydrogels, the snapping of hydrogel sheets can be programmed to achieve different structures and actuation behaviors. We have developed theoretical model to elucidate the crucial role of dual gradients and predict the snapping motion of various hydrogel materials. This new design principle provides guidance for fabricating actuation materials with applications in tissue engineering, soft robotics, and active medical implants.

INTRODUCTION

Shape transformation is ubiquitous in living systems, such as prey capture action by carnivorous plants (*1*, *2*). These natural phenomena have been sources of inspiration for engineering functional shape-transforming materials (*3*, *4*). Among others, responsive hydrogels capable of shape transformation under various stimuli have attracted tremendous interests due to their promising applications in soft robotics (*5*, *6*), drug delivery (*7*), tissue engineering (*8*), microfluidics (*9*), and so on (*10*–*12*). Typical responsive polymers used for designing shape-transforming materials include poly(*N*,*N*-dimethylaminoethyl methacrylate) (PDMAEMA) and poly(*N*-isopropylacrylamide) (PNIPAM), which are thermoresponsive (i.e., the gels swell/deswell reversibly in response to temperature variation around the critical phase transition temperature) (*12*–*14*). The shape transformation of hydrogels largely relies on the differential swelling of hydrogels in different regions of the materials. The in-plane and/or out-of-plane mismatch in volume change drives the gradual shape evolution of hydrogels to take various shapes (*13*–*21*). Currently, the majority of efforts at this frontier are centered on enhancing the complexity of shapes that can be acquired by hydrogels and on diversifying the responsiveness of hydrogels to external stimuli (*22*–*26*).

In nature, the leaves of the Venus flytrap can rapidly close up to capture insects in one-tenth of a second, a behavior distinct from that of the typically gradual and relatively slow shape transformation of hydrogels (Fig. 1A) (*2*). The extremely rapid motion of this plant is believed to associate with the accumulation and quick release of energy (*27*). Mimicking this sudden yet discontinuous motion is essential to the development of ultrafast actuators with broad applications (e.g., in soft robots). The few existing approaches to achieve this type of motion are usually based on reversible switching between concave and convex structures of bistable polymeric sheets, which only allows for limited complexity in structures and actuation behaviors (*28*–*30*). Nevertheless, there is still a great need for new design principles of snapping motion of responsive materials.

Here, we report a nature-inspired design of responsive hydrogel sheets with the capability of accumulating elastic energy and rapidly releasing the energy through ultrafast snapping deformation. Our experimental results and theoretical model suggest that the snapping motion of hydrogel materials originate from the dual-gradient structural design of the hydrogels. When reduced graphene oxide (rGO)/PDMAEMA composite hydrogel sheets with dual-gradient structures are used as a model system, we demonstrate that the sheets can accumulate elastic energy by converting prestored thermal or chemical energy and rapidly snap (<1 s) in a reverse direction to release the elastic energy in response to external stimuli (Fig. 1). The snapping velocity, angle, and location of the sheet can be tuned by modulating the magnitude and location of prestored energy within the hydrogel. As a result, the hydrogel sheets can be programmed and snapped to achieve different structures and actuation behaviors. The new design principle of snapping deformation is general and applicable to other materials, such as neat hydrogels or elastomers. This work provides guidance for fabricating actuation materials with applications in tissue engineering, soft robotics, and active implants.

RESULTS

We used an rGO/PDMAEMA composite hydrogel sheet with dual gradients (i.e., chain and cross-linking density gradients) along the thickness direction as an exemplary system for demonstration of our concept (Fig. 2A). The composite hydrogel was fabricated by ultraviolet (UV)–induced free radical generation of GO to initiate polymerization of DMAEMA (monomer) and *N*,*N*′-methylene-bis-acrylamide (MBA; cross-linking agent) (fig. S1). A mixture of GO, DMAEMA, and MBA (in the absence of conventional photoinitiator) was filled in-between a sealed space and irradiated by UV light. The strong UV absorption by GO led to the gradient formation of light intensity along the thickness direction of the mixture (fig. S2A) (*22*, *31*, *32*). The higher UV intensity at the UV-exposed side causes the generation of a higher concentration of free radicals on the surface of GOs (*33*), thus a faster polymerization of both the DMAEMA and MBA at this side (*22*, *31*). As a result, the UV-exposed side (denoted as the HD side) has the higher chain density and cross-linking density of PDMAEMA than the other side (denoted

[1]State Key Laboratory of Bio-fibers and Eco-textiles, Shandong Collaborative Innovation Center of Marine Biobased Fibers and Ecological Textiles, College of Materials Science and Engineering, Institute of Marine Biobased Materials, Qingdao University, Qingdao 266071, China. [2]Department of Chemistry and Biochemistry, University of Maryland, College Park, MD 20892, USA. [3]State Key Laboratory of Molecular Engineering of Polymers, Department of Macromolecular Science, Fudan University, Shanghai 200438, China.
*These authors contributed equally to this work.
†Corresponding author. Email: sky@qdu.edu.cn (K.S.); znie@fudan.edu.cn (Z.N.)

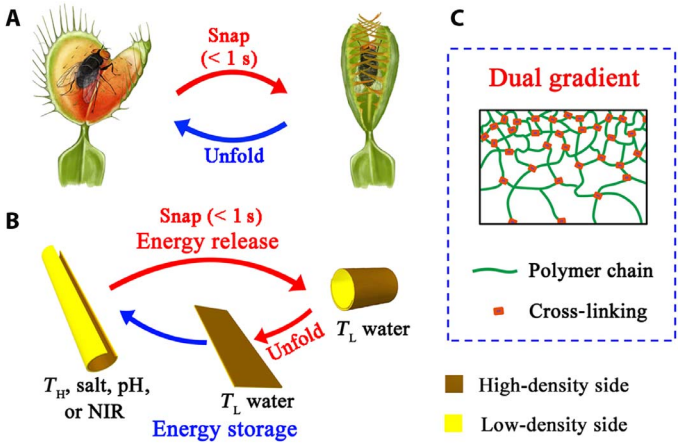

Fig. 1. Illustrative scheme of the snapping deformation. (**A**) Snapping of the Venus flytrap. (**B**) Inverse snapping of a dual-gradient hydrogel sheet. (**C**) A carton showing the cross section of a dual-gradient hydrogel.

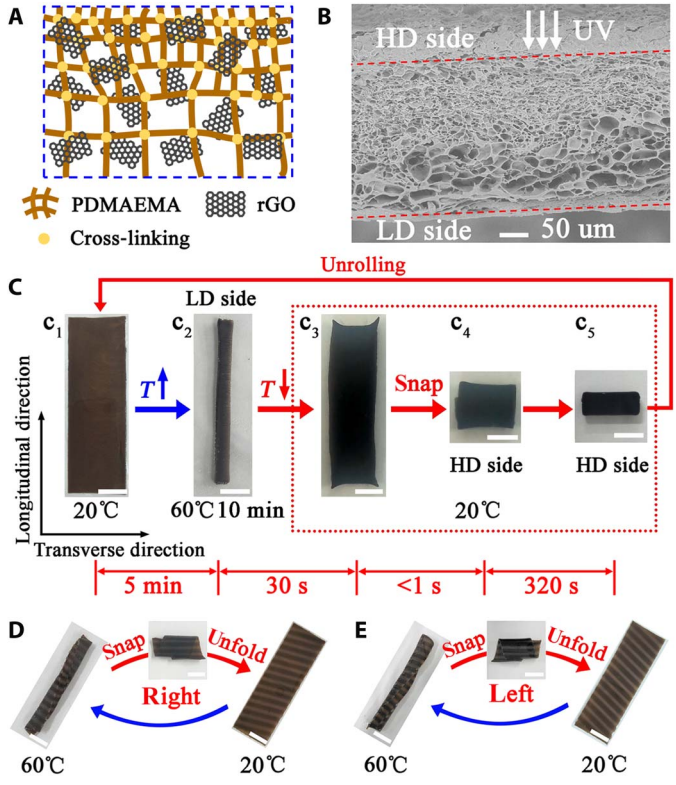

Fig. 2. Inverse snapping of dual-gradient rGO/PDMAEMA hydrogel sheets. (**A** and **B**) Schematic illustration (A) and cross-sectional SEM image (B) of the dual-gradient structure of rGO/PDMAEMA hydrogel sheets. (**C**) Shape transformation of the sheets in response to temperature variation. (**D** and **E**) Inverse snapping of the sheets with strip patterns to form chiral structures with controlled handedness. Scale bars, 1 cm (C and D).

as the LD side) (Fig. 2A). The existence of chain density gradient and cross-linking density of the hydrogel was confirmed by a combination of tools including scanning electron microscopy (SEM), confocal laser scanning microscopy (CLSM), x-ray photoelectron spectroscopy (XPS), and Raman spectra (see more detailed discussion in section S3).

When submerged from 20°C water into water with 60°C higher than its volume phase transition temperature (fig. S3A), the originally flat composite sheet curved up toward the HD side along the longitudinal axis into a tubular structure in ~2 min due to the high shrinkage rate of the HD side [Fig. 2C (c_2) and fig. S3, B and C]. It is notable that when placed back into the 20°C water, instead of following an exactly reverse pathway of original shape transformation, the hydrogel sheet took a completely different route in which a new intermediate state appeared. It first unrolled until bending angle decreased to ~43° in 30 s and then rapidly snapped (as fast as below 1 s) in a reverse direction along the transverse axis, associated with a sharp increase in bending angle from 38° to 540° [Fig. 2C (c_3 and c_4), fig. S3D, and movie S1]. The process was followed by a period (~320 s) of continuous rolling to further increase the bending angle to a maximal value of 1089° [Fig. 2C (c_5) and fig. S3D]. Last, this inversely snapped structure gradually unrolled to be flat in ~60 min (fig. S3E). The snapping axis direction of the sheets can be regulated by patterning dual-gradient regions into the sheets (fig. S4, A and B). As an example, patterning the hydrogels with left- and right-titled stripes using a mask during UV irradiation enabled the snapping of hydrogels along predefined axial direction to form chiral structures with left- and right-handedness (Fig. 2, D and E, and movie S2). Notably, the inverse snapping of hydrogels can occur for dual-gradient hydrogels with arbitrary initial shapes (fig. S4, C and D). Tuning the initial shape of hydrogels allows for controlling the initial curling configurations of hydrogels and hence the manner of subsequent inverse snapping of hydrogels.

The inverse snapping of hydrogel sheets constitutes a new mechanism of energy transformation, as illustrated in Fig. 3A. When placed back into low-temperature (T_L) water, the curled sheet obtained at high temperature (T_H) unrolls due to the higher swelling rate of the HD side. During this process, the longitudinal expansion of the HD side relative to the LD side first eliminates the axial shrinkage stress at the HD side and then generates cumulative expansion stress (i.e., elastic energy) at the HD side [Fig. 3A (a_1 and a_2)]. The accumulated axial expansion stress cannot be released because of the constraint caused by curling along the longitudinal axis, until the bending angle of the curled hydrogel decreases to a threshold value. At this moment, the stress at the HD side can be released instantaneously, leading to abruptly inverse snapping of the sheet [Fig. 3A (a_2 and a_3)]. Subsequently, the bending angle increases gradually until the HD side reaches swelling equilibrium [Fig. 3A (a_3 and a_4)]. Eventually, the inverse-snapped structure unrolls gradually as the LD side of the hydrogel sheet swells. Notably, the instantaneous release of accumulated elastic energy during snapping can induce quick jumping of hydrogels in 20°C water (fig. S4E and movie S3).

The energy conversion involved in the snapping process can be divided into three stages: (i) conversion of part of the prestored thermal/chemical effective energy (E^*) into cumulative elastic energy during unrolling of the curled sheet, (ii) instantaneous release of accumulated elastic energy (E') in the form of snapping, and (iii) gradual release of the rest energy (E'') to further curl the sheet after snapping. These energies can be correlated through a simple equation

$$E^* = E' + E'' \quad (1)$$

The variation of T_H (i.e., the initial temperature for stimulating the gel) affects not only the original deformation of the hydrogel sheet at this temperature but also its later inverse snapping deformation when the gel was subsequently immersed in water at T_L. This indicates that E^* can be modulated by controlling the initial T_H used to stimulate the curling of hydrogels (Fig. 3, B and C, and S5). We

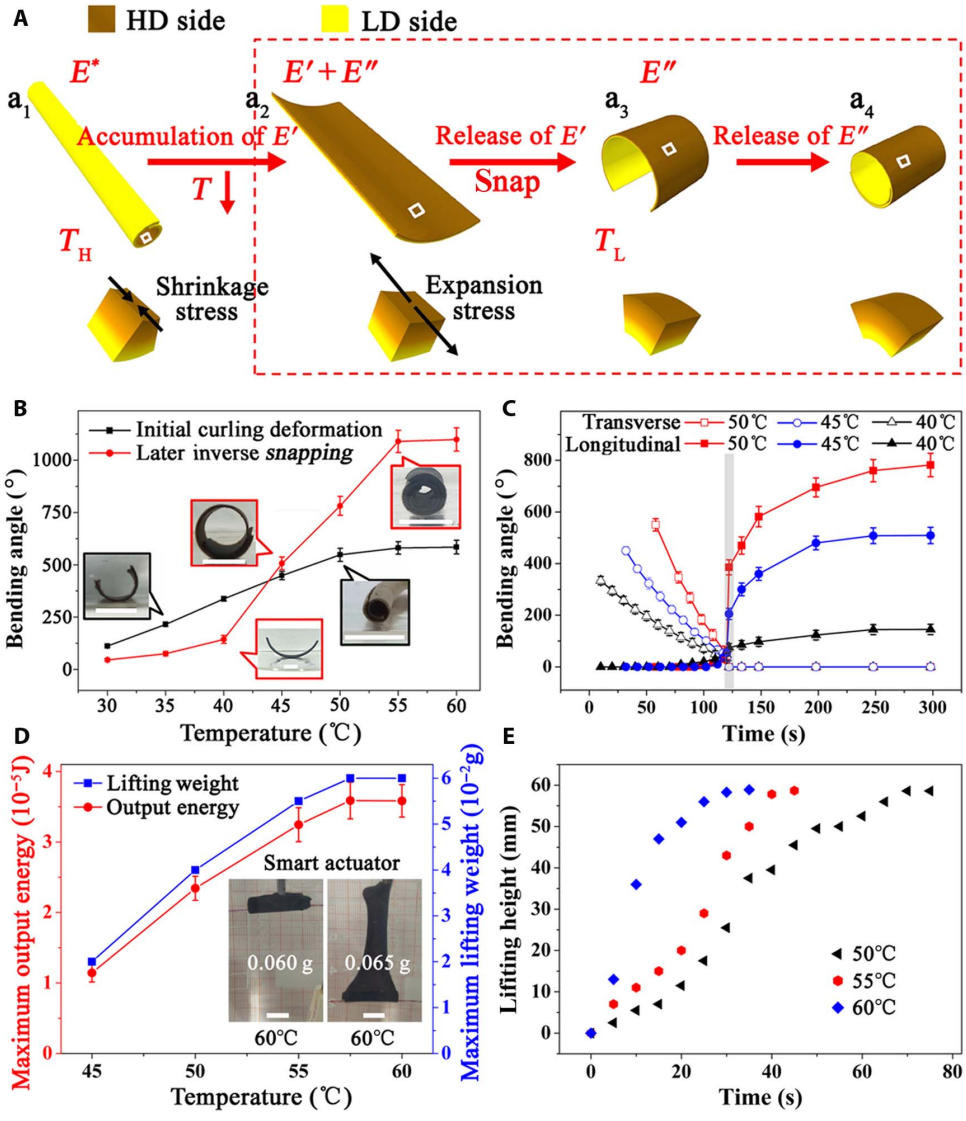

Fig. 3. Programmable inverse snapping enabled by energy prestored within dual-gradient composite hydrogel sheets. (**A**) Schematic illustration of inverse snapping of composite hydrogel sheets when moved from T_H to T_L. (**B**) Maximum bending angles of initial curling of hydrogel sheets at different T_H (black curve) and corresponding inverse snapping of the sheets in 20°C water (red curve). The gel sheets initially curved toward the HD side when they were stimulated in water with different T_H for 10 min. When the curved sheets prestored with energy were subsequently immersed in 20°C water, the sheets snapped inversely depending on the T_H for pretreatment. (**C**) Kinetics of snapping at 20°C for sheets initially treated at different T_H. For comparison, the onset time of snapping for all cases was set to the same value. (**D**) Maximum output energy and lifting weight at 20°C by the same hydrogel sheet after energy storage at different T_H. Optical images in the insets show the lifting of 0.06- and 0.065-g iron wires by the snapping of the same hydrogel sheet. The gel was pretreated at 60°C and then immersed in 20°C water to trigger snapping deformation. (**E**) Height of lifting 0.04-g object at 20°C by hydrogel treated at different T_H as a function of lifting time. Scale bars, 1 cm.

clarify that the pretreatment time used for energy storage for all stimuli in this article is 10 min, unless otherwise noted. Both E^* and E' increase with increasing T_H, leading to an increased bending angle and snapping velocity in 20°C water (Fig. 3, B and C, fig. S5, eqs. S11 to S13, and a comparison of snapping velocity between movies S1 and S4). As such, the snapping of sheets can be quantitatively programmed by tuning the magnitude of prestored energy using different T_H. This is further confirmed by their self-regulated actuation capability when the snapping of prestimulated hydrogel sheets was used to actuate the weight lifting in 20°C water (fig. S5D). The maximum lifting weight (i.e., output energy) in 20°C water by the same sheets increased with the increase in initial T_H (Fig. 3D). The same trend was observed for the lifting velocity of the hydrogel when the same weight was lifted (Fig. 3E and movies S5 and S6). The concept of modulating the storage and release of energy in hydrogels enables the design of intelligent materials with programmable motion, mass identification, and power regulation.

The snapping behaviors of hydrogels can be modulated by stimulating the gel with pH and ion strength (IS) variation, owing to the weak polyelectrolyte nature of PDMAEMA (fig. S6). Similar to T_H stimulation, the hydrogel sheet rolled up toward the HD side to store energy in response to an increase in IS or addition of base and quickly snapped to release the energy in a reverse direction when placed in 20°C water (fig. S6 and movie S7). It is worth noting that the inverse snapping of hydrogel sheets can occur in a broad range of external stimuli, such as T_L of

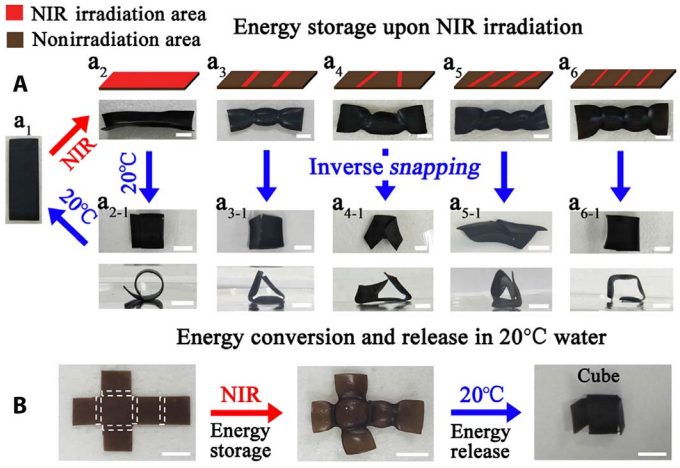

Fig. 4. Transformation of a dual-gradient composite hydrogel sheet into complex shapes by programming energy prestorage. (**A**) Inverse snapping of a composite hydrogel sheet in 20°C water after NIR irradiation regionally of the sheet in air. (**B**) Programmable folding of a composite hydrogel sheet into a cube in 20°C water after NIR irradiation of the highlighted regions in air. Scale bars, 1 cm.

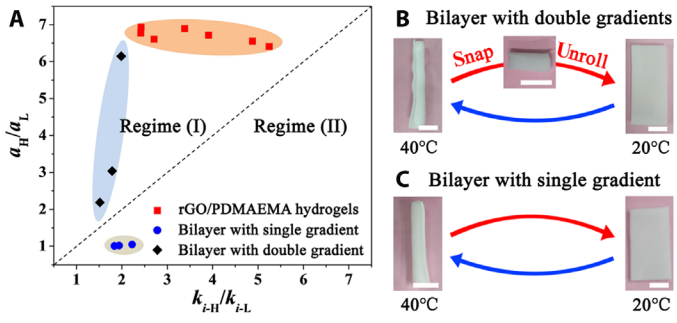

Fig. 5. General criterion for inverse snapping of hydrogel sheets. (**A**) Production diagram of various hydrogel sheets: composite hydrogel sheets under different initial T_H, bilayer PNIPAM hydrogel sheets with different dual gradients, and bilayer hydrogel sheets with different single gradients. The regimes (I) and (II) correspond to the condition of $a_H/a_L > k_{i\text{-}H}/k_{i\text{-}L}$ (snapping) and $a_H/a_L < k_{i\text{-}H}/k_{i\text{-}L}$ (no snapping), respectively. (**B** and **C**) Deformation of different bilayer hydrogel sheets under the stimuli of 20° and 40°C: double gradients (B) and single gradient (C). Scale bars, 1 cm.

0° to 35°C, weak IS, and strong acid and base (fig. S6 and movie S8 to S10). This overcomes the limitation of narrow operating conditions for conventional responsive hydrogels (e.g., with lower critical solution temperature).

Furthermore, the composite hydrogels are responsive to near-infrared (NIR) light due to the photothermal effect of rGOs (*25*). In response to localized NIR irradiation in the air, the hydrogel sheet bent exclusively toward the HD sides regardless of the irradiation side due to the original dual gradients [Fig. 4A (a_2) and fig. S7]. Submerging the NIR-irradiated hydrogel sheet into 20°C water can also induce its inverse snapping [Fig. 4A (a_{2-1})]. Notably, NIR light enabled local energy storage and, hence, controllable inverse snapping of hydrogel sheets to produce various complex structures under constant stimulating conditions (Fig. 4A and movies S11 and S12). As an example, we showed programmable folding of gel sheet into a cube by controlling the location of light exposure and energy storage within the sheet (Fig. 4B). Such programmable materials have great potential in biomedicine (e.g., for minimally invasive surgery) and soft robotics (*34*).

We quantitatively analyzed the snapping process and established a general criterion for inverse snapping as follows (see detailed explanation in eqs. S1 to S10)

$$\frac{a_H}{a_L} > \frac{k_{i-H}}{k_{i-L}} \quad (2)$$

where a_H and a_L are the expansion rates of the HD and LD sides for the curled hydrogel sheet in 20°C water, respectively, and $k_{i\text{-}H}$ and $k_{i\text{-}L}$ are the transverse shrinkage ratios of the HD and LD sides after initial curling, respectively.

Equation 2 suggests that the inverse snapping of the hydrogel sheet is attributed to its dual-gradient structure. The polymer chain density gradient imparts the hydrogel sheet with high expansion rate ratio (a_H/a_L), while the higher cross-linking density of the HD side inhibits the shrinkage/deswelling of the hydrogel sheet more than the LD side (*32*), leading to a relative small value of $k_{i\text{-}H}/k_{i\text{-}L}$ of the two sides. Two types of gradient structures together give $a_H/a_L > k_{i\text{-}H}/k_{i\text{-}L}$, as confirmed by the presence of all data points of snapping composite hydrogels (calculated from fig. S8, A and B) in regime (I) in Fig. 5A.

The general criterion of inverse snapping we derived was further verified by comparing the deformation behaviors of bilayered PNIPAM hydrogel sheets with dual gradients (in both polymer density and cross-linking density) and with only cross-linking density, respectively. The dual-gradient PNIPAM sheets exhibited inverse snapping motions, whereas all the single-gradient hydrogels only showed simple bending in response to thermal stimulations (Fig. 5, B and C, and movies S13 and S14). The values of a_H/a_L and $k_{i\text{-}H}/k_{i\text{-}L}$ of these hydrogels (calculated from fig. S8, C and D) fell into the corresponding regions of the diagram in Fig. 5A.

DISCUSSION

In summary, we have demonstrated a general principle for the design of hydrogel materials with energy transformation ability to trigger programmable snapping deformation. By controlling the magnitude and location of energy prestorage within hydrogels, the inverse snapping deformations of the hydrogels can be programmed to achieve different actuations and structures. The energy transformation–induced snapping of hydrogels is attributed to their dual-gradient structure (i.e., polymer chain density gradient and cross-linking density gradient). A theoretical model was proposed to interpret and predict the snapping of hydrogels, which is in good agreement with our experimental observations. Moreover, the dual-gradient hydrogel can directly work as a self-propelled actuator with the ability of weight identification and power control under constant stimuli. This research provides new insights into the actuation of materials and practical guidance for the design and fabrication of autonomous actuators, soft robotics, and active implants.

MATERIALS AND METHODS

Materials

DMAEMA (99%, purified through a column of alkaline alumina to remove the inhibitor before use), MBA (99%), NIPAM (>98%), *N*, *N*,*N*′,*N*′-tetramethylethylenediamine (TEMED; 99%), ammonium

peroxodisulfate, sodium fluorescein (>99%), and rhodamine 6G (99%) were purchased from Aladdin Reagents Co. (Shanghai, China). Pure water was obtained by deionization and filtration using a Millipore purification apparatus (resistivity > 18.2 megohm·cm). GO was prepared from graphite powder by the modified Hummers method. The size and thickness of the GO sheets (fig. S9) used in this study are ~0.6 to 2.6 μm and ~1.1 nm, respectively.

Fabrication of dual-gradient rGO/PDMAEMA hydrogel sheets

The rGO/PDMAEMA composite hydrogel was synthesized by using UV-induced free radical generation of GO to initiate the polymerization of a mixture of DMAEMA, GO, and MBA. Briefly, DMAEMA (monomer, 0.214 ml), MBA (photocrosslinker, 20 mg), and 0.8 weight % (wt %) GO (0.4 g) were added into 0.7 ml of distilled water. After ultrasonic dispersion for about 15 min, the solution was rapidly injected into a laboratory-made mold, which consisted of two glass substrates separated by a 0.5-mm spacer. This mold was then exposed to UV light (15 W, 254 nm) for 8 hours (fig. S1). After polymerization, the as-prepared rGO/PDMAEMA hydrogel sheet was immersed in bulk deionized water for about 48 hours to remove impurities or unpolymerized monomers.

Fabrication of dual-gradient bilayer PNIPAM hydrogel sheets

The HD layer (with high chain density of PNIPAM and high cross-linking density) was first prepared by a free radical polymerization. During this process, 0.2 to 0.4 g of NIPAM and 0.03 g of MBA were added into 1.8 ml of distilled water. After the addition of 3 μl of TEMED and 0.2 g of ammonium persulfate solution (1 wt %), the polymerization was carried out at room temperature in a sealed vessel for 4 hours. The LD layer (with low chain density of PNIPAM and low cross-linking density) was then prepared directly on the top of the HD layer using similar procedures. To reduce the chain density and the cross-linking density of PNIPAM, the amounts of NIPAM and MBA in this process were decreased to 0.1 and 0.006 g, respectively. Each layer of the PNIPAM hydrogel sheets has a thickness of 360 μm.

Fabrication of single cross-linking gradient bilayer PNIPAM hydrogel sheets

The layer with high cross-linking density (HC side) was first prepared. During this process, 0.3 g of NIPAM and 0.03 g of MBA, 3 μl of TEMED, and 0.2 g of ammonium persulfate solution (1 wt %) were added into 1.8 ml of distilled water. After polymerization, the new layer with low cross-linking density (LC side) was directly prepared on the HC layer. To lower the cross-linking density, the MBA for this layer was decreased to 0.0075–0.015 g.

Experimental procedures for the actuation of hydrogel sheets

All the experiments of hydrogel deformation were carried out in a petri dish with a diameter of 150 mm. The temperature of the system was controlled by a thermal-magnetic heater (MS-H-Pro, Scilogex, USA). The pH of the solution was measured by a pH meter (FiveEasy Plus, METTLER TOLEDO, USA). An 808-nm laser (MDL-N-808, Changchun New Industries Optoelectronics Technology Co. Ltd, China) was used as the light source, and a power of 2 W/cm^2 was used in all the experiments. During the deformation, the hydrogel sheet was first pretreated under the stimuli of T_H, IS, pH, or NIR for 10 min and then immersed in 20°C water or other stimuli for inverse snapping deformation. Note that when NIR was used for local pretreatment, each pattern was irradiated for 2 min rather than 10 min.

Characterization

The cross-sectional morphologies of the as-prepared hydrogel sheet were observed by SEM (JSM-6390LV, JEOL) operated at 15.0 kV. The sample for SEM imaging was prepared by fracturing the freeze-dried hydrogel in liquid nitrogen and gold sputtering on the fracture surface. To confirm the gradient structure, the cross-sectional morphologies of the samples dyed by the dilute solution of sodium fluorescein (~10^{-6} M) and rhodamine 6G (~10^{-6} M) were respectively imaged by using CLSM (Nikon A1R plus, Tokyo, Japan) with an exciting wavelength of 488 nm in the single-channel mode. Raman scattering measurements were performed using a Raman system (inVia-reflex, Renishaw) with confocal microscopy under an excitation light of 514.5 nm. Atomic force microscopy (AFM) images were taken by an atomic force microscope (Agilent Technologies Inc.) operating in tapping mode using silicon cantilevers with ~300-kHz resonance frequency. The surface chemical constitutions of the hydrogel sheets were characterized by XPS (Thermo Fisher Scientific, ESCALAB 250).

SUPPLEMENTARY MATERIALS

Supplementary material for this article is available at http://advances.sciencemag.org/cgi/content/full/5/4/eaav7174/DC1

Section S1. Theoretical derivation of inverse snapping
Section S2. Energy transformation during the inverse snapping
Section S3. Characterization of dual-gradient rGO/PAMAEMA hydrogel sheet
Fig. S1. Schematic illustration of the fabrication process of the GO/PDMAEMA hydrogel sheet.
Fig. S2. Characterization of dual-gradient rGO/PAMAEMA hydrogel sheet.
Fig. S3. Temperature-dependent swelling ratio and deforming kinetics.
Fig. S4. Shape transformations of hydrogel sheets with different patterns and initial shapes.
Fig. S5. Dependence of inverse snapping on T_H.
Fig. S6. Demonstration of the multiresponsive feature.
Fig. S7. NIR irradiation–triggered shape transformation.
Fig. S8. a_H, a_L, $k_{i\text{-}H}$, and $k_{i\text{-}L}$ for different hydrogel sheets.
Fig. S9. AFM characterization of GO.
Movie S1. Inverse snapping of hydrogel sheet submerged from 60°C into 20°C water.
Movie S2. Inverse snapping of patterned hydrogel sheet.
Movie S3. Jumping and somersaulting motion.
Movie S4. Inverse snapping of hydrogel sheet submerged from 40°C into 20°C water.
Movie S5. Lifting processes of hydrogel actuator after energy storage at 60°C.
Movie S6. Lifting processes of hydrogel actuator after energy storage at 50°C.
Movie S7. Inverse snapping of hydrogel sheet submerged from 5 M NaCl into 20°C water.
Movie S8. Inverse snapping of hydrogel sheet submerged from 60°C into 0°C water.
Movie S9. Inverse snapping of hydrogel sheet submerged from 60°C into 35°C water.
Movie S10. Inverse snapping of hydrogel sheet submerged from 5 M NaCl into 0.1 M NaCl.
Movie S11. Local energy storage upon NIR irradiation.
Movie S12. Local energy release to induce triangle shape deformation.
Movie S13. Inverse snapping of dual-gradient bilayer PNIPAM hydrogel sheet.
Movie S14. Inverse snapping of single-gradient bilayer PNIPAM hydrogel sheet.

REFERENCES AND NOTES

1. S. Armon, E. Efrati, R. Kupferman, E. Sharon, Geometry and mechanics in the opening of chiral seed pods. *Science* **333**, 1726–1730 (2011).
2. H. Ko, A. Javey, Smart actuators and adhesives for reconfigurable matter. *Acc. Chem. Res.* **50**, 691–702 (2017).
3. O. M. Wani, H. Zeng, A. Priimagi, A light-driven artificial flytrap. *Nat. Commun.* **8**, 15546 (2017).
4. J. Deng, J. Li, P. Chen, X. Fang, X. Sun, Y. Jiang, W. Weng, B. Wang, H. Peng, Tunable photothermal actuators based on a pre-programmed aligned nanostructure. *J. Am. Chem. Soc.* **138**, 225–230 (2016).
5. L. Ionov, Hydrogel-based actuators: Possibilities and limitations. *Mater. Today* **17**, 494–503 (2014).

6. Y. Zhang, J. Liao, T. Wang, W. Sun, Z. Tong, Polyampholyte hydrogels with pH modulated shape memory and spontaneous actuation. *Adv. Funct. Mater.* **28**, 1707245 (2018).
7. K. Malachowski, J. Breger, H. R. Kwag, M. O. Wang, J. P. Fisher, F. M. Selaru, D. H. Gracias, Stimuli-responsive theragrippers for chemomechanical controlled release. *Angew. Chem. Int. Ed. Engl.* **53**, 8045–8049 (2014).
8. D. Seliktar, Designing cell-compatible hydrogels for biomedical applications. *Science* **336**, 1124–1128 (2012).
9. S. Haefner, P. Frank, M. Elstner, J. Nowak, S. Odenbach, A. Richter, Smart hydrogels as storage elements with dispensing functionality in discontinuous microfluidic systems. *Lab Chip* **16**, 3977–3989 (2016).
10. Y. S. Zhang, A. Khademhosseini, Advances in engineering hydrogels. *Science* **356**, eaaf3627 (2017).
11. W. Luo, Q. Cui, K. Fang, K. Chen, H. Ma, J. Guan, Responsive hydrogel-based photonic nanochains for microenvironment sensing and imaging in real time and high resolution. *Nano Lett.*, 10.1021/acs.nanolett.7b04218 (2018).
12. C. Ma, W. Lu, X. Yang, J. He, X. Le, L. Wang, J. Zhang, M. J. Serpe, Y. Huang, T. Chen, Bioinspired anisotropic hydrogel actuators with on–off switchable and color-tunable fluorescence behaviors. *Adv. Funct. Mater.* **28**, 1704568 (2018).
13. T. Manouras, E. Koufakis, S. H. Anastasiadis, M. Vamvakaki, A facile route towards PDMAEMA homopolymer amphiphiles. *Soft Matter* **13**, 3777–3782 (2017).
14. S. H. Yuk, S. H. Cho, S. H. Lee, pH/temperature-responsive polymer composed of poly((*N*,*N*-dimethylamino)ethyl methacrylate-*co*-ethylacrylamide). *Macromolecules* **30**, 6856–6859 (1997).
15. Z. L. Wu, M. Moshe, J. Greener, H. Therien-Aubin, Z. Nie, E. Sharon, E. Kumacheva, Three-dimensional shape transformations of hydrogel sheets induced by small-scale modulation of internal stresses. *Nat. Commun.* **4**, 1586 (2013).
16. D. Morales, B. Bharti, M. D. Dickey, O. D. Velev, Bending of responsive hydrogel sheets guided by field-assembled microparticle endoskeleton structures. *Small* **12**, 2283–2290 (2016).
17. E. Palleau, D. Morales, M. D. Dickey, O. D. Velev, Reversible patterning and actuation of hydrogels by electrically assisted ionoprinting. *Nat. Commun.* **4**, 2257 (2013).
18. H. Thérien-Aubin, Z. L. Wu, Z. Nie, E. Kumacheva, Multiple shape transformations of composite hydrogel sheets. *J. Am. Chem. Soc.* **135**, 4834–4839 (2013).
19. J. Kim, J. A. Hanna, M. Byun, C. D. Santangelo, R. C. Hayward, Designing responsive buckled surfaces by halftone gel lithography. *Science* **335**, 1201–1205 (2012).
20. S.-J. Jeon, A. W. Hauser, R. C. Hayward, Shape-morphing materials from stimuli-responsive hydrogel hybrids. *Acc. Chem. Res.* **50**, 161–169 (2017).
21. Y. Liu, J. Genzer, M. D. Dickey, "2D or not 2D": Shape-programming polymer sheets. *Prog. Polym. Sci.* **52**, 79–106 (2016).
22. J. Guo, T. Shroff, C. Yoon, J. Liu, J. C. Breger, D. H. Gracias, T. D. Nguyen, Bidirectional and biaxial curving of thermoresponsive bilayer plates with soft and stiff segments. *Extrem. Mech. Lett.* **16**, 6–12 (2017).
23. H. Thérien-Aubin, M. Moshe, E. Sharon, E. Kumacheva, Shape transformations of soft matter governed by bi-axial stresses. *Soft Matter* **11**, 4600–4605 (2015).
24. A. W. Hauser, A. A. Evans, J.-H. Na, R. C. Hayward, Photothermally reprogrammable buckling of nanocomposite gel sheets. *Angew. Chem. Int. Ed.* **54**, 5434–5437 (2015).
25. C. Ma, X. Le, X. Tang, J. He, P. Xiao, J. Zheng, H. Xiao, W. Lu, J. Zhang, Y. Huang, T. Chen, A multiresponsive anisotropic hydrogel with macroscopic 3D complex deformations. *Adv. Funct. Mater.* **26**, 8670–8676 (2016).
26. X. Peng, C. Jiao, Y. Zhao, N. Chen, Y. Wu, T. Liu, H. Wang, Thermoresponsive deformable actuators prepared by local electrochemical reduction of poly(*N*-isopropylacrylamide)/graphene oxide hydrogels. *ACS Appl. Nano Mater.* **1**, 1522–1530 (2018).
27. Y. Forterre, J. M. Skotheim, J. Dumais, L. Mahadevan, How the Venus flytrap snaps. *Nature* **433**, 421–425 (2005).
28. Q. Zhao, X. X. Yang, C. Ma, D. Chen, H. Bai, T. Li, W. Yang, T. Xie, A bioinspired reversible snapping hydrogel assembly. *Mater. Horiz.* **3**, 422–428 (2016).
29. D. P. Holmes, A. J. Crosby, Snapping surfaces. *Adv. Mater.* **19**, 3589–3593 (2007).
30. H. Lee, C. Xia, N. X. Fang, First jump of microgel; actuation speed enhancement by elastic instability. *Soft Matter* **6**, 4342–4345 (2010).
31. H. Kim, S. J. Lee, Stomata-inspired membrane produced through photopolymerization patterning. *Adv. Funct. Mater.* **25**, 4496–4505 (2015).
32. M. J. Motala, D. Perlitz, C. M. Daly, P. Yuan, R. G. Nuzzoet, K. J. Hsia, Programming matter through strain. *Extrem. Mech. Lett.* **3**, 8–16 (2015).
33. A. S. Nia, W. H. Binder, Graphene as initiator/catalyst in polymerization chemistry. *Prog. Polym. Sci.* **67**, 48–76 (2017).
34. X. Hu, J. Zhou, M. Vatankhah-Varnosfaderani, W. F. M. Daniel, Q. Li, A. P. Zhushma, A. V. Dobrynin, S. S. Sheiko, Programming temporal shape shifting. *Nat. Commun.* **7**, 12919 (2016).

Acknowledgments

Funding: This work was supported by the National Natural Science Foundation of China (51573080 and 51403113), the Key Research and Development Project of Shandong Province (2016GGX102005), and the China Postdoctoral Science Foundation (2017M622132).

Author contributions: K.S. and Z.N. proposed and supervised the project. Z.N., K.S., W.F., C.S., and H.G. designed and performed the experiments and wrote the paper. J.S., R.W., and R.Z. participated in most of the experiments. All authors have given approval to the final version of the manuscript. **Competing interests:** The authors declare that they have no competing interests. **Data and materials availability:** All data needed to evaluate the conclusions in the paper are present in the paper and/or the Supplementary Materials. Additional data related to this paper may be requested from the authors.

Submitted 13 October 2018
Accepted 26 February 2019
Published 19 April 2019
10.1126/sciadv.aav7174

Citation: W. Fan, C. Shan, H. Guo, J. Sang, R. Wang, R. Zheng, K. Sui, Z. Nie, Dual-gradient enabled ultrafast biomimetic snapping of hydrogel materials. *Sci. Adv.* **5**, eaav7174 (2019).

Science Advances

Dual-gradient enabled ultrafast biomimetic snapping of hydrogel materials

Wenxin Fan, Caiyun Shan, Hongyu Guo, Jianwei Sang, Rui Wang, Ranran Zheng, Kunyan Sui and Zhihong Nie

Sci Adv **5** (4), eaav7174.
DOI: 10.1126/sciadv.aav7174